Efficient first-principles method for calculating the circular dichroism of nanostructures

Francisco Hidalgo, A. Sánchez-Castillo, and Cecilia Noguez*
Instituto de Física, Universidad Nacional Autónoma de México, Apartado Postal 20-364, México D.F. 01000, México
(Received 2 January 2009; revised manuscript received 29 January 2009; published 24 February 2009)

A first-principles method is developed to study the natural optical activity of nanostructures, making large-scale calculations of electronic circular dichroism feasible. Expressions to calculate circular dichroism using density-functional theory for finite and periodic systems are obtained and implemented within the SIESTA program package. To show the versatility and applicability of the method, the circular dichroism of the high fullerenes C_{76} and C_{78} is investigated. The results for these fullerenes show good consistency with previous semiempirical calculations, and a very good agreement with experiments. The method is generalized to treat periodic structures such as nanotubes, and the circular dichroism of the carbon single-wall nanotube (4,2) is studied, and the spectrum is interpreted in terms of its electronic density of states. It is found that the calculated circular dichroism spectra can be used to discriminate among different nanostructures through optical activity experiments. It is concluded that this methodology provides theoretical support for the quantification, understanding, and prediction of chirality and its measurement in nanostructures. It is expected that this information would be useful to motivate further experimental studies and the interpretation of natural optical activity in terms of the electronic circular dichroism in nanostructures.

DOI: 10.1103/PhysRevB.79.075438 PACS number(s): 78.67.Bf, 78.67.Ch, 78.20.Bh, 78.20.Ek

I. INTRODUCTION

Since the discovery of natural optically active substances by Arago nearly two centuries ago,[1] physicists, chemists, biologists, and material scientists have been fascinated with their study. Optical activity is the physical phenomenon associated to the rotation of linearly polarized light when it propagates through chiral compounds. Chirality is a geometrical property where a figure, or group of points, whose ideally realized image in a plane mirror cannot be brought to coincide with itself. Despite of the simplicity of its definition, chirality is important in physics, chemistry, and biology, and today, we know that left-amino acids, left peptides, and right sugars are predominant in the living world, and practically all natural products, such as proteins, lipids, nucleic acids, hormones, vitamins, antibiotics, and many drugs manifest optical activity.[1–3] This is why chirality plays a major role in biochemistry and pharmacology, and today it becomes an important issue in nanoscience and nanotechnology.[4] For instance, nanoscale materials are used for asymmetric catalysis,[5] enantiomeric analysis,[6] enantioselective separation,[7] and also as molecular devices, such as chiral supramolecules,[8] self-assembled nanotubes,[9] chiral fullerenes,[10] chiral carbon nanotubes,[11] DNA technology,[12] and so on. In fact, nearly all aspects of chiral technology, including synthesis, separation, and analysis, have already seen nanoscale approaches. Whether the goal is to use nanostructures for new approaches to solving problems in chiral technology or to use molecular chirality to engineering useful properties in nanoscale materials, this area is fruitful and exciting and certainty to continue to attract interest for the years to come.

Although chiral structures are mostly organic molecules, it is known that inorganic nanostructures such as fullerenes and nanotubes also do.[13] Additionally, optical activity has been observed recently in a new class of metallic materials at the nanometric scale. Specifically, circular dichroism (CD) signals have been measured in ligand-protected metal nanoclusters and nanoparticles when chiral ligands were used. Schaaff and Whetten[14] did the first observation of this kind in 2000, by measuring intense optical activity in giant gold-glutathione nanocluster compounds. These results not only provided evidence for the existence of novel optically active nanomaterials, but also indicated that chiral effects are present in matter at the nanoscale. Since 2003, there have been published several additional reports confirming the observation of optically active nanoparticles using distinct chiral adsorbates as protecting ligands of Au, Ag, and Pd nanoclusters.[15,16] Recently, a chiral metallic cluster core model has been provided by recent developments on the total structure determination of a large gold-thiolate cluster compound.[17] Additionally, recent reliable theoretical and experimental evidence proves the existence of intrinsically bare chiral gold nanoclusters with sizes between 20–100 atoms, for which optical activity has been predicted.[18–20]

Applications of chiral molecules and nanostructures in biological systems can be hampered by the fact that there are two possible isomers depending on the handedness of the object: left-handed (LH) and right-handed (RH). These isomers that are nonsuperimposable complete mirror images of each other, are called enantiomers. In a symmetric or achiral environment, enantiomers have identical chemical and physical properties except for their ability to rotate the linearly polarized light by equal amounts but in opposite directions. Therefore, a mixture of equal parts of an isomer and its enantiomer, termed racemic mixture, shows a zero net rotation of the plane-polarized light. Energetically, the isomer and its enantiomer have the same probability to coexist, therefore, racemic mixtures are usually synthesized in the laboratory, unless an asymmetric procedure to unbalance the process is achieved, the latter resulting in a substance with nonzero optical activity. The enrichment of a single enantiomer is a very important issue, and much of the attention has been directed to their synthesis and/or separation, in a so-called enantioselectivity process. RH and LH enantiomers often do

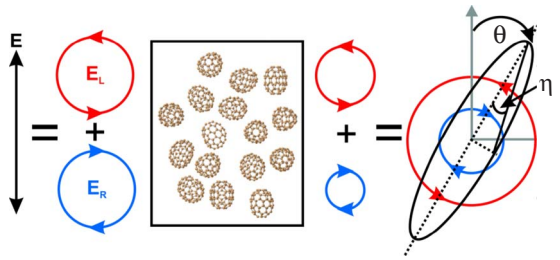

FIG. 1. (Color online) Schematic model of a linearly polarized electromagnetic field (E) composed by the sum of left (E_L) and right (E_R) circularly polarized light that is traveling in an absorbing medium made of a collection of randomly oriented chiral nanoparticles. The system absorbs differently L and R circularly polarized light, presenting the circular dichroism phenomenon, and resulting in an elliptical polarized beam.

have different chemical properties related to other substances that are also enantiomers. Since many molecules in the bodies of living beings are enantiomers themselves, there is often a marked difference in the effects of two symmetrical enantiomers, and their characterization is a very important issue.[1–3]

To characterize chirality and other related effects there are available chiroptical techniques such as electronic circular dichroism, which detect slight differences in absorption between left and right circularly polarized light existing in chiral molecules. First-principles methods capable of quantify and predict CD in nanostructures are highly desirable, and some attempts have been done in this direction.[21] However, *ab initio* and time-dependent density-functional theory (TD-DFT) methods are still too expensive to be applied to large nanostructures, compromising accuracy, and computational efficiency. In this work, we show that by using density-functional theory (DFT) is good enough to understand and predict CD in terms of the atomic and electronic structures of systems with sizes in the nanometer scale. Here, we have developed quantum-mechanical expressions to calculate the CD based on a linear combination of atomic orbitals within the time-dependent perturbation theory based in DFT. We test our method and compare with previous semiempirical results for chiral high fullerenes, finding good consistency. Then, we show the applicability of our method, where an excellent agreement with experiments is found. The method is also adapted to treat periodic systems, and carbon nanotubes are studied. Finally, we discuss the potentiality of our method for applications to other complex nanostructures.

II. THEORY

Optical activity is the ability of substances to rotate the plane of polarization of linearly polarized light passing through them. Linearly polarized light can be seen as the superposition of left (L) and right (R) circularly polarized light (see Fig. 1), as

$$E_{\mu/\nu} = \mathbf{E}_R \pm \mathbf{E}_L = E_0 e^{i(\mathbf{k}\cdot\mathbf{r}-\omega t)}\{(\hat{n}_\mu + i\hat{n}_\nu) \pm (\hat{n}_\mu - i\hat{n}_\nu)\}, \tag{1}$$

where μ and ν denote Cartesian coordinates, and E_0 is the amplitude of the incident electromagnetic field of wave vector $\mathbf{k}$ and frequency ω. When light passes through an absorbing optically active system, the chiral compound absorbs differently L and R circularly polarized light. This phenomenon is known as electronic circular dichroism and is defined as the absorption difference between L and R circularly polarized light, as

$$\Delta A(\omega) = \kappa_L(\omega) - \kappa_R(\omega), \tag{2}$$

where $\kappa(\omega)$ is the absorption index. Considering the corresponding L(R)-circularly polarized electromagnetic field, it becomes

$$E_{L(R)}(\omega) = E_0 e^{-2\pi\kappa_{L(R)}(\omega)l/\lambda}, \tag{3}$$

where l is the optical path length, and λ is the wavelength of the incident electromagnetic light. Since $\kappa_L(\omega) \neq \kappa_R(\omega)$ when linearly polarized light passes through an absorbing optically active system, light becomes elliptically polarized, as shown in Fig. 1. It is possible to define a quantity named ellipticity, $\eta(\omega)$, in terms of the minor and major axes of the projected ellipse in the plane perpendicular to the propagation vector of the outgoing light, such as

$$\tan\ \eta(\omega) = \frac{E_R(\omega) - E_L(\omega)}{E_R(\omega) + E_L(\omega)} = \tanh\left\{\frac{\pi l}{\lambda}[\kappa_L(\omega) - \kappa_R(\omega)]\right\}, \tag{4}$$

and for small ellipticities,

$$\eta(\omega) \approx \frac{\pi l}{\lambda}[\kappa_L(\omega) - \kappa_R(\omega)], \tag{5}$$

i.e., it is proportional to CD, which was defined in Eq. (2).

In a system composed of N particles per unit volume, the absorption index can be written in terms of the molar extinction, ε, for a given concentration, ϕ, of chiral molecules, considering

$$4\pi\kappa(\omega) = 2.303\lambda\phi\varepsilon(\omega), \tag{6}$$

where λ is in centimeters. Finally, CD is usually given in terms of the difference of the L and R molar extinctions in moles per liter, such that

$$\Delta\varepsilon(\omega) = \varepsilon_L(\omega) - \varepsilon_R(\omega), \tag{7}$$

which is given in liters mol^{-1} cm^{-1}, which is a quantity independent of the specific concentration of the sample.

To fully characterize and understand the CD spectra of optically active chiral nanoparticles, we need to find the macroscopic quantity in Eq. (7) from quantum-mechanical calculations. Long time ago, Rosenfed and others[1,22,23] gave the first steps in this direction and developed the theoretical foundations of CD. Here, we review briefly the main concepts to obtain CD from quantum-mechanical calculations, following the text by Barron.[1] Rosenfeld demonstrated, using time dependent perturbation theory, that the electric-dipole moment induced by a frequency-dependent electromagnetic field on a chiral molecule may be written as[23]

$$\vec{\mu}_{\mathrm{mol}}(\omega) = \alpha(\omega)\mathbf{E}(\omega) + \beta(\omega)\frac{\partial \mathbf{B}(\omega)}{\partial t}, \tag{8}$$

with $\mathbf{E}$ and $\mathbf{B}$ the applied electric and magnetic fields, respectively. Here $\alpha(\omega)$ is the tensor that denotes the usual dipole polarizability whose imaginary part is related to linear light absorption, and $\beta(\omega)$ is a tensor related to the specific rotation, whose imaginary part gives the rotational strength of optically active systems.[21]

The macroscopic CD, given by the difference of the L and R molar extinction of a system of N chiral molecules randomly oriented that are under the action of an external electromagnetic field, is related to the rotational strength in terms of the $\beta(\omega)$ as[1]

$$\Delta\varepsilon(\omega) = \frac{0.1343 \times 10^{-5}}{3300}\beta(\omega)\tilde{\nu}^2, \tag{9}$$

where $\tilde{\nu}(\mathrm{cm}^{-1})$ is the wave number, and

$$\beta(\omega) = -\frac{1}{3\omega}\mathrm{Tr}\{\mathrm{Re}[\tilde{G}_{\mu\nu}(\omega)]\}, \tag{10}$$

which has units of a_0^4, with a_0 the Bohr radius (in atomic units), and Re means the real part. The above expression was obtained from a time-dependent perturbation theory, where the Hamiltonian was expressed through an electromagnetic multipolar expansion of the vector $\mathbf{A}(\mathbf{r},t)$, and scalar $\phi(\mathbf{r},t)$ potentials,[24] where $\mathbf{r}$ denotes position and t means time. Then, the average over the isotropic system of randomly oriented chiral particles was considered, where chiral particles means particles with no mirror planes, centers of inversion or other no improper axes of rotation. The latter gave CD in terms of the trace of $\tilde{G}_{\mu\nu}$. This tensor is expressed as[1]

$$\tilde{G}_{\mu\nu}(\omega) = \frac{1}{\hbar}\sum_{n\neq 0}\left\{\frac{\langle 0|\hat{\mu}_\mu|n\rangle\langle n|\hat{m}_\nu|0\rangle}{\omega_{n0} - \omega - i\gamma_{n0}} + \frac{\langle 0|\hat{m}_\nu|n\rangle\langle n|\hat{\mu}_\mu|0\rangle}{\omega_{n0} + \omega + i\gamma_{n0}}\right\}, \tag{11}$$

and is associated to both electric-dipole, $\hat{\mu}$, and magnetic-dipole, $\hat{m}$, quantum operators. These are defined by

$$\hat{\mu} = q\mathbf{r}, \quad \text{and} \quad \hat{m} = \frac{q}{2m}\mathbf{r}\times\hat{\mathbf{p}}, \tag{12}$$

where q and m are the electron's charge and mass, respectively; and $\hat{\mathbf{p}}$ is the linear momentum operator. The matrix elements $\langle 0|\mu_\mu|n\rangle$ and $\langle n|m_\nu|0\rangle$ correspond to transitions from the ground state $|0\rangle$ with energy $\hbar\omega_0$, to the excited state $|n\rangle$ with energy $\hbar\omega_n$, where $|n\rangle$ and $|0\rangle$ are the eigenfunctions of the unperturbed Hamiltonian, and $\omega_{n0}=\omega_n-\omega_0$. Moreover, γ_{n0} is the dephasing rate between eigenstates, which is normally taken to be zero on the assumption that the field frequency is far from resonance, while in the resonant region it needs to be taken different from zero. The computation of the tensor in Eq. (11) involves the summation over the excited states, but most quantum calculations of $\beta(\omega)$ avoid this approach in practice by invoking a linear-response formalism.[25] In contrast, we consider the complete summation over occupied and empty states of the basis set considered here. As follows, we develop expressions to calculate Eq. (11) using DFT.

The precise knowledge of the atomic configuration existing in the optically active compound under consideration, as well as a reliable methodology to obtain their electronic structure, including ground and excited states are necessary. Although significant progress has been achieved during the last few years in the field of computational nanoscience to implement methods able to address the above issues, it had not been possible to evaluate accurately the CD spectra of nanostructures from first-principles calculations. The main reason has been related with the huge computational resources necessary to perform structural optimizations, electronic structure calculations, and chiroptical properties quantification using, for example, DFT and/or TDDFT calculations. Additionally, the electronic structure model used to compute the tensor of Eq. (11) must satisfy the origin invariance of the CD in the limit of a complete basis set, which is fulfilled by the following commutation rule:[21]

$$[\mathbf{r},\hat{H}] = \frac{i\hbar}{m}\hat{\mathbf{p}}. \tag{13}$$

In particular, the last equation is satisfied by the DFT formalism. Therefore, we have implemented the computation of CD in Eq. (9) within the SIESTA computer code,[26,27] which is a versatile DFT program to perform *ab initio* electronic structure calculations and quantum molecular-dynamics simulations of molecules and solids. It uses the standard Kohn-Sham self-consistent density-functional method in the local-density approximation (LDA) or generalized-gradient approximation (GGA), norm-conserving pseudopotentials in its fully nonlocal form, atomic orbitals as basis set, allowing unlimited multiple-zeta and angular momenta, polarization, and off-site orbitals. Additionally, simulations with SIESTA of several hundred atoms are feasible with modest computational resources.

In our implementation within SIESTA for molecules and finite nanostructures, first we rewrite the matrix elements of Eq. (11) by using the definitions of the operators from Eqs. (12), as

$$\langle 0|\mu_\mu|n\rangle\langle n|m_\nu|0\rangle = \frac{q^2}{2m}\langle 0|r_\mu|n\rangle\langle n|(\mathbf{r}\times\hat{\mathbf{p}})_\nu|0\rangle,$$

$$\langle 0|m_\nu|n\rangle\langle n|\mu_\mu|0\rangle = \frac{q^2}{2m}\langle 0|(\mathbf{r}\times\hat{\mathbf{p}})_\nu|n\rangle\langle n|r_\mu|0\rangle. \tag{14}$$

Assuming the completeness of the basis set, $\Sigma_n|u\rangle\langle u| = 1$, and evaluating Eq. (13) as, $\langle n|p_\mu|0\rangle = -im\omega_{n0}\langle n|r_\mu|0\rangle$,[28] the diagonal terms to calculate the trace of tensor $\tilde{G}_{\mu\nu}(\omega)$ are given as

$$\tilde{G}_{\mu\mu}(\omega) = \frac{q^2}{2\hbar}\sum_{n\neq 0,u}\gamma_{n0}\left[\frac{\omega_{0u}R'_{\mu\mu}}{(\omega_{n0}-\omega)^2+\gamma_{n0}^2} - \frac{\omega_{un}R''_{\mu\mu}}{(\omega_{n0}+\omega)^2+\gamma_{n0}^2}\right], \tag{15}$$

where

$$R'_{\mu\mu} = \langle 0|r_\mu|n\rangle[\langle n|r_\nu|u\rangle\langle u|r_\gamma|0\rangle - \langle n|r_\gamma|u\rangle\langle u|r_\nu|0\rangle],$$

$$R''_{\mu\mu} = [\langle 0|r_\nu|u\rangle\langle u|r_\gamma|n\rangle - \langle 0|r_\gamma|u\rangle\langle u|r_\nu|n\rangle]\langle n|r_\mu|0\rangle.$$

Now, replacing the expression for $\tilde{G}_{\mu\mu}(\omega)$ into Eqs. (10) and (9), one obtains the CD for finite systems.

On the other hand, to implement the formalism for periodic systems such as nanotubes, we use the velocity representation of the electric-dipole moment,

$$\langle 0|p_\mu|n\rangle = -\frac{im}{q}\omega_{n0}\langle 0|\hat{\mu}_\mu|n\rangle, \tag{16}$$

such that, tensor $\tilde{G}_{\mu\nu}(\omega)$ is now given by

$$\tilde{G}_{\mu\nu} = \frac{iq}{m\hbar}\sum_{n\neq 0}\frac{1}{\omega_{n0}}\left\{\frac{\langle 0|p_\mu|n\rangle\langle n|m_\nu|0\rangle}{(\omega_{n0}-\omega)^2+\gamma_{n0}^2} - \frac{\langle 0|m_\nu|n\rangle\langle n|p_\mu|0\rangle}{(\omega_{n0}+\omega)^2+\gamma_{n0}^2}\right\}. \tag{17}$$

Under periodic boundary conditions is better representing wave functions of the periodic system in terms of the momenta of the particles rather than positions. So that making use of Eq. (13) again, we have

$$\tilde{G}_{\mu\mu}(\omega) = \frac{-q^2}{2m^3\hbar}\sum_{n\neq 0,u}\frac{\gamma_{n0}}{\omega_{n0}}\left[\frac{P'_{\mu\mu}}{\omega_{un}[(\omega_{n0}-\omega)^2+\gamma_{n0}^2]} - \frac{P''_{\mu\mu}}{\omega_{0u}[(\omega_{n0}+\omega)^2+\gamma_{n0}^2]}\right], \tag{18}$$

with

$$P'_{\mu\mu} = \langle 0|p_\mu|n\rangle[\langle n|p_\nu|u\rangle\langle u|p_\gamma|0\rangle - \langle n|p_\gamma|u\rangle\langle u|p_\nu|0\rangle],$$

$$P''_{\mu\mu} = [\langle 0|p_\nu|u\rangle\langle u|p_\gamma|n\rangle - \langle 0|p_\gamma|u\rangle\langle u|p_\nu|n\rangle]\langle n|p_\mu|0\rangle.$$

Finally, one replaces the last expression for $\tilde{G}_{\mu\mu}(\omega)$ into Eqs. (10) and (9) to obtain the CD for a periodic system.

In this work, we consider electronic transitions over all occupied and unoccupied states, which are generated by an extended-function basis set that assures convergence of the chiroptical effects. In particular, we employed scalar relativistic norm-conserving pseudopotentials,[29] a double-zeta polarized basis set,[27] the local-density approximation as well as the generalized-gradient approximation with the Perdew-Burke-Ernzerhof (PBE) parametrization.[30] We also assume that the dephasing rate between eigenstates is the same for all the eigenstates, $\hbar\gamma_{n0}=0.05$ eV. In Sec. III, we study chiral clusters and nanotubes to show the versatility and accuracy of our method, which can be applied to large-scale systems, as we will show.

III. APPLICATION TO FINITE NANOSTRUCTURES: THE CASE OF HIGH FULLERENES

Among nanostructures, fullerenes are well known to be chiral.[10] Despite their simple atomic structure, the physical and chemical properties depend dramatically on their chirality. Increasing the size of fullerenes, the number of allowed constitutional isomers also does dramatically and so does the number of chiral representatives. For example, 14 out of the 19 isomers of the C_{86} fullerene are chiral, while C_{76} has only two isomers, where one is chiral and the other is not; and C_{78} has five isomers and where only one is chiral.[10] In contrast, C_{60} has only one isomer that is achiral. To measure optical activity in these compounds, it is necessary the enrichment or separation of a single enantiomer, named enantiomeric purity or excess (*ee*). In such case, the resulting substance has nonzero optical activity, and it can be characterized using, for instance, circular dichroism. As larger *ee* is attained, the CD intensity increases, where a maximum is reached when *ee* =100%. This has been the case for the fullerenes C_{76} and C_{78}, where some *ee* has been obtained by using high-performance liquid chromatography to separate enantiomers, and where there are already experimental CD spectra, which are useful to compare with our results and show the viability and confidence of our code for finite large-scale systems.

First, we investigate the fullerene C_{60} that belongs to the icosahedral point group and has a large amount of symmetry operations including plane mirrors. Therefore, it is an achiral cluster that we can use as a reference system. The atomic structures of fullerenes have been taken from Ref. 31, and have been relaxed using the SIESTA code.[26,27] In the case of C_{60}, the electronic CD spectrum shows an almost null signal (not shown here), consistently with achiral structures. Small features are observed that are associated to numerical errors, which are smaller than 0.01%, as compare to CD of equivalent chiral fullerenes. Therefore, we have confirmed that CD is null for achiral systems, and that the numerical errors are very small.

Right after the discovery of the fullerene C_{60},[32] the search for new allotropic forms of carbon conducted to the synthesis and isolation of the so-called higher fullerenes:[33] C_{76}, C_{84}, C_{90} y C_{94}. After their characterization, by employing mass spectrometry, ^{13}C nuclear magnetic resonance, electronic absorption (ultraviolet visible) and vibrational (infrared) spectroscopy, these all-carbon molecules were termed as higher fullerenes.[33] Later, it was possible to separate two of the three possible isomers of the C_{78} by using high-performance liquid chromatography,[34,35] which enables enantiomeric separations by using a chiral phase, which gives different affinities between the enantiomers. In the same way, the fullerene C_{76}, which was predicted to be chiral[36] with a D_2 symmetry, consisting of a spiralling, double-helical arrangement of edge-sharing pentagons and hexagons, was also isolated.[37] After that, Hawkins and co-workers[38,39] observed optical activity by measuring CD on these fullerenes. Here, we study CD of C_{76} and C_{78}, which are well characterized systems. In Fig. 2, the different isomers of C_{76} and C_{78} are shown.

A. Optical activity of C_{76}

The fullerene C_{76} has two constitutional isomers, one belongs to the symmetry group T_d, and then it is achiral. The other isomer has a D_2 symmetry and then is chiral, as can be seen in Fig. 2. For the achiral fullerene, again a null CD is obtained (not shown here), where we find that the numerical errors are of the same order of magnitude as those discussed above for C_{60}. On the other hand, the CD spectrum of the D_2

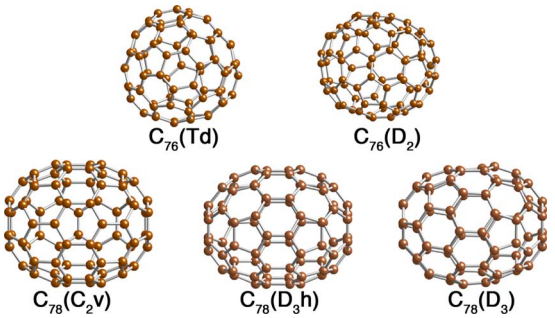

FIG. 2. (Color online) Atomic models of the two different isomers of C_{76} and the three isomers of C_{78}. The isomers in the right-hand side for both sizes are chiral.

isomer shows optical activity, as seen in experimental measurements.[38,40,41] In 1993 Hawkins and Meyer[38] achieved the unbalance of the racemic mixture of C_{76} fullerenes with D_2 symmetry dispersed in toluene, by using asymmetric osmylation and high-performance liquid chromatography. In that work they reported a CD spectrum that showed a well-defined line shape between 1.5 and 4 eV.[38] Later, Kessinger *et al.*[40] prepared enantiomerically pure C_{76} with a general electrochemical method for the removal of methano bridges from methanofullerenes by using the Retro-Bingel reaction. They also measured CD of this fullerene suspended in toluene in the same energy region, between 1.5 and 4 eV, finding good agreement with the previous results of Hawkins and Meyer.[38]

Goto *et al.*[41] investigated experimentally and theoretically the optical activity of the fullerene C_{76}. In this case, they measured CD in a larger spectroscopic region from 1.5 to 5.5 eV, finding good agreement with previous measurements.[38,40] They calculated the CD of the D_2 isomer of C_{76} by employing the π-electron SCF-CI-DV MO (self-consistent field-configuration interaction-dipole velocity molecular orbital) method. However, the calculation is difficult for fullerenes within this scheme because the atomic structure is distorted in such a way that nonplanar $\pi \rightarrow \pi^*$ transitions have to be computed. Therefore, they parametrized the integrals associated to the dipolar resonances, fitting them to provide the best comparison with experiments. This is, they used a semiempirical SCF method to calculate the CD spectrum where only transitions among π states were considered.[41] In contrast, we perform a first-principles calculations that consider an extended basis set where all the transitions between electron states are taken into account and not parametrizations are done. Although the semiempirical SCF approximation gave good results as compared with experiments,[38,40] some details of the CD spectra were not well reproduced, as can be seen in Fig. 3. Additionally, since the integrals were parametrized for this particular case, the semiempirical SCF method is not able to predict results for other fullerenes.

In Fig. 3, we compare the CD data taken from the experiments of Goto *et al.*[41] with their semiempirical SCF calculation and our DFT calculated CD spectrum. A shift to higher energies of ~0.6 eV of the semiempirical SCF results was found as compared with the experimental data, which Goto *et al.*[41] attributed to their methodology. However, they did not considered that the fullerenes in the experiments were

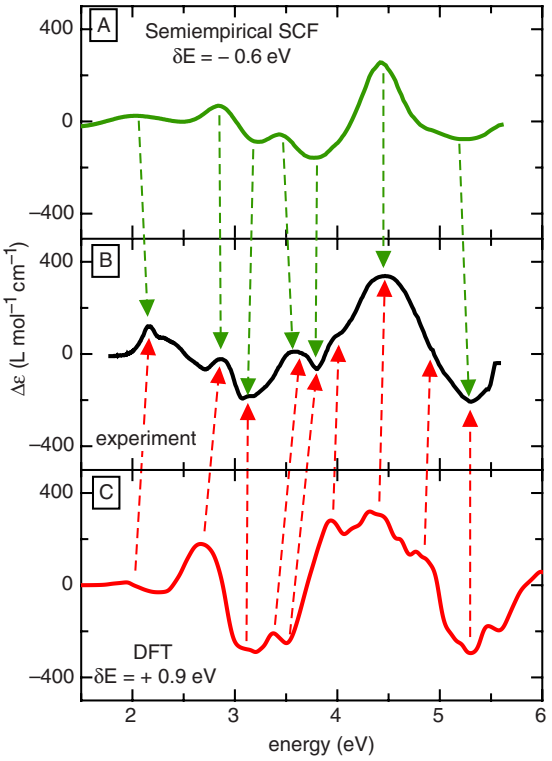

FIG. 3. (Color online) CD spectra of the D_2 isomer of C_{76}. (a) Semiempirical SCF calculations from Ref 41. The spectrum was shifted −0.6 eV. (b) Experimental data also taken from Ref. 41. (c) Our DFT calculated CD spectrum with a Gaussian broadening of 0.4 eV. The spectrum was shifted +0.9 eV. The arrows are used to indicate the correspondence between the main peaks of both calculated CDs with the experimental curve.

suspended in toluene and thus, the experimental optical response could be redshifted with respect to those of the same fullerenes in vacuum.[42] On the other hand, the DFT curve is redshifted by about 0.9 eV. This is expected since DFT always underestimates the optical gap. In Fig. 3, the semiempirical SCF result and our DFT spectrum are redshifted (−0.6 eV) and blueshifted (+0.9 eV), respectively, for a better comparison with the experimental data. Both CD calculations, DFT and semiempirical SCF, show in general good agreement with measurements, where the intensities and line shapes of the experimental spectrum are well described by both calculations. Since the overall calculated and measured intensities are similar, one can conclude that the enantiomeric excess or purity of the experimental sample is large, as it was claimed.[40]

In Fig. 3(a), we can observe that the semiempirical SCF calculation shows a symmetriclike intense narrow peak at about 4.4 eV, with a small minimum at around 5.3 eV, contrary to the experimental CD, whose peak at ~4.4 eV is nonsymmetric, wider, and exhibits a shoulder at around 4 eV. Additionally, the experimental minimum at 4.3 eV is deeper than the calculated one. On the other hand, the DFT curve resembles better the width of the mayor peak at 4.4 eV, has another peak at around 3.9 eV that corresponds to the experimental shoulder at 4 eV, and the minimum at 4.3 eV has the same relative intensity that the experimental one. At smaller

energies both calculations fail to reproduce the intensity of the experimental spectrum, as it happens for the measured peak at 2.1 eV. Also, the negative structure at 2.8 eV in the experimental CD results to be positive in both calculations. These discrepancies in intensity and sign could be assigned to different factors, for instance, to the toluene effect in the fullerene optical absorption, to the separation procedure where some residua from the removal of methano bridges from methanofullerenes could be still present, or possibly to some other factors as temperature effects and so on. The DFT result shows more structure in the peaks than the SCF calculations since all the allowed transitions are taken into account. On the other hand, the semiempirical SCF curve is smoother since only $\pi-\pi*$ transitions were accounted. We consider that the agreement between experiments and DFT is very good, as it is also the case for C_{78}, as we discuss below, and as for C_{84}, as it would be discussed elsewhere.[43]

B. Optical activity of C_{78}

As we have already explained, the isomers D_3h and C_2v of the fullerene C_{78} are achiral. This fact was confirmed with our CD calculations, where the signals found were null (not shown here). Again, the numerical errors were found to be of the same magnitude as for C_{60}. Experimental CD was reported by Hawkins *et al.*,[39] which again achieved the unbalance of the racemic mixture of C_{78} with D_3 symmetry dispersed in toluene by using asymmetric osmylation and high-performance liquid chromatography. In this work they reported the CD that shows a well-defined line shape between 1.5 and 4 eV.[39] However, one should notice that now the intensity of the experimental spectrum is about 40 times smaller than the one for C_{76}, but it is large enough that the numerical errors associated to our calculations are still smaller. Probably, the enantiomeric separation process was not efficient to achieve a large *ee*, as we discuss later.

In Fig. 4, the experimental electronic CD measured by Hawkins *et al.*[39] is shown, as well as the DFT calculated CD spectrum. Again our results are blueshifted, now by 0.4 eV, for a better comparison with the experimental data. Additionally, we have also multiplied the DFT calculated CD spectrum by a factor of 1/30 to fit the intensity of the experimental data. The difference on the intensity can be attributed to the purity or excess of the enantiomeric mixture. On the other hand, the line shape of the experimental and DFT calculated CD spectra shows a remarkable agreement. A maximum at around 3.5 eV, as well as the two minima at about 2.6 and 4 eV, respectively, is found in both spectra. Also, the alternate negative-positive structure from 1.5 to about 2.3 eV is well represented. Differences in the intensity of some peaks are found, for instance, the negative peak at 3.1 eV. These differences can be attributed again to several different factors, as the effect of solution where the fullerenes are dispersed, temperature effects that can make the peaks wider and hampered some electronic transitions, as well as some residual molecules that can be attached to the fullerenes and can change significantly the spectrum. In any case, we consider that the agreement between theory and experiment is excellent.

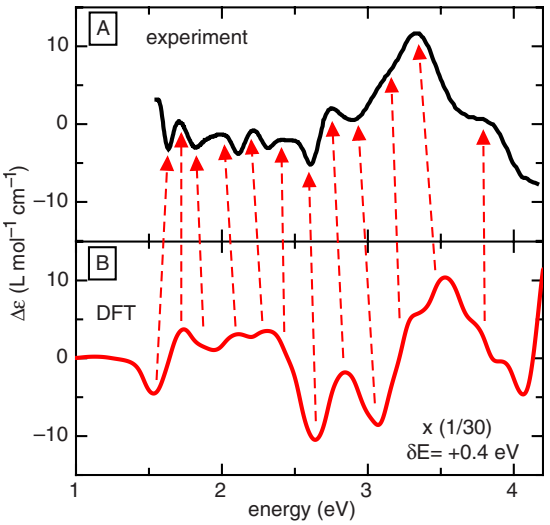

FIG. 4. (Color online) CD spectra of the D_3 isomer of C_{78}. (a) Experimental data taken from Ref. 39. (b) Our DFT calculated CD spectrum with a Gaussian broadening of 0.2 eV. The calculated spectrum was shifted +0.4 eV and multiplied by a factor of 1/30 for a better comparison with the experimental curve. The arrows are used to indicate the correspondence of the main peaks between both CDs.

Semiempirical quantum-mechanical calculation for the fullerene C_{78} was previously reported.[44] The authors found a shift of about +0.4 eV of the theoretical spectrum with respect to the experimental curve, again, we believe that this difference can be attributed to the effect of the solution where the fullerenes are immersed.[42] The semiempirical quantum-mechanical method was not able to give a resolution on the units, such that, they were not able to compare the intensity of their spectrum with the experimental curve. Also, they did not found the rich peak structure reported experimentally and reproduced here using DFT, they only found a structure of three peaks, where the big discrepancies were attributed to the "nonperfect simulation of the linewidth or to the value of the selected line broadening for the blow up.[44]"

Finally, we would like to further comment on the discrepancy of the intensity between the experimental curve and the calculated CD spectrum of C_{78}. As we have already explained, this discrepancy can be attributed to the low *ee* of the experimental sample. In fact, the same effect has been also observed in the case of the fullerene C_{84}, where the calculated spectra[43,45,46] are of the same order of magnitude of that reported here, while the experimental data[47] are about 15 times smaller. The theoretical spectra were calculated using different approaches, TDDFT, semiempirical SCF, and DFT, respectively.[43,45,46] and all of they coincided. In fact, we have calculated the CD for two different chiral D_2 isomers of the high fullerenes C_{92} and C_{100}, and the intensity of the spectra is again of the same order of magnitude as for the other fullerenes, as shown in Fig. 5. One important fact that one should notice by inspecting the spectra for all the fullerenes reported here is that the CD is very sensitive to each size, and for a given size, to each isomer.[43] Therefore, CD can be a powerful technique to characterize these chiral

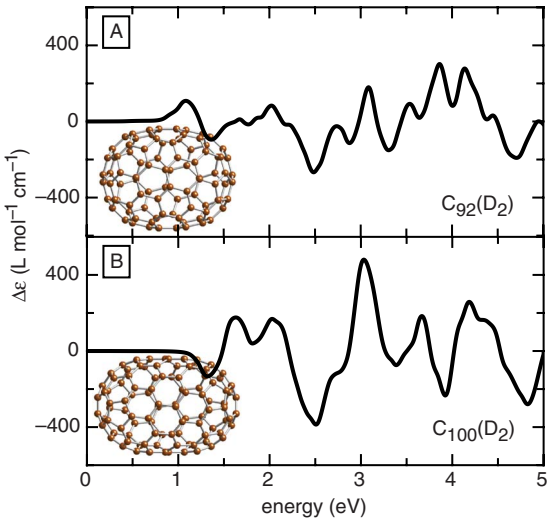

FIG. 5. (Color online) DFT calculated CD spectra of one of the D_2 isomers of (a) C_{92} and (b) C_{100}, with a Gaussian broadening of 0.2 eV. The atomic models of both fullerenes are also shown.

nanostructures when a confident theoretical interpretation can be done, as the one presented here.

IV. APPLICATION TO PERIODIC NANOSTRUCTURES: THE CASE OF THE CARBON SINGLE-WALL NANOTUBE (4,2)

Carbon single-wall nanotubes (SWNTs) resemble the wrapping of a sheet of carbons located in a two-dimensional hexagonal lattice called graphene. The sheet can be rolled up in different ways to form a cylinder, such that, the graphene lattice along the nanotube axis shows a helical twist defining its chirality.[13] Despite of their simple atomic structure, the properties of SWNTs depend dramatically on their chirality. The chirality and diameter of SWNTs are specified using the chiral vector, $\vec{C}_h$, which is determined by the unit vectors of the hexagonal lattice $\vec{a}_1$ and $\vec{a}_2$, as

$$\vec{C}_h = n\vec{a}_1 + m\vec{a}_2, \tag{19}$$

where n and m are integers numbers. These pair of numbers define how the graphene sheet is rolled up, such that, SWNTs with different (n,m) can have the same diameter, $|\vec{C}_h|/\pi$, but different chirality.

In general, there are three different classes of SWNTs: (i) the armchair with $n=m\neq 0$, (ii) the zigzag nanotube with $n\neq m$, and $m=0$, and (iii) chiral nanotubes with $n\neq m$ and $m\neq 0$. The first two types of SWNTs are achiral, while the third one is chiral. For any circumferential length, $|\vec{C}_h|$, can be only two possible achiral nanotubes, while the number of possible chiral SWNTs isomers substantially increases as $|\vec{C}_h|$ does. Therefore, most nanotubes are intrinsically chiral. The two mirror-related forms of SWNTs, right and left handed, depend on which way one rolls up the graphene sheet. For instance, one can either curl the edges up and over to form a tube with (n,m), or curl down and under forming a (m,n) tube. Therefore, the nanotube with indices (m,n) is the enantiomer of the one with indices (n,m). Additionally, the optical activity originating from SWNTs has been theoretically predicted.[48–50]

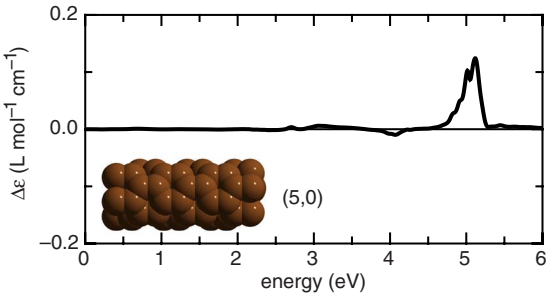

FIG. 6. (Color online) CD spectrum of the zigzag, then, achiral SWNT (5,0), where numerical errors smaller than 0.1% are observed. The atomic model of SWNT (5,0) is also shown.

The selected synthesis, separation, and enrichment of a single enantiomer has been a very important issue since the discovery of carbon nanotubes.[51,52] Some synthesis methods have been developed, which limit the chiralities of SWNTs,[53] and enhance and separate metallic from semiconducting SWNTs.[54–60] Then, the separation based on length, diameter, and/or chirality can be attained using chromatography.[61–63] The concentration of each SWNT is usually an unknown variable, and the isomer and its enantiomer are still present in a racemic mixture. However, it was not until very recently that the unbalance and enantiomeric separation or *ee* has been conducted, such that, optical activity has been observed in samples containing SWNTs.[64–66] However, the unknown final concentrations for each (n,m),[65,66] the presence of other chiral molecules,[64] and/or other factors, make accurate theoretical work absolutely necessary for the interpretation of the CD spectra.

Here, we investigate the optical activity of SWNTs by using the second part of the formalism of Sec. II. First, we investigate the optical activity of achiral nanotubes to look at the accuracy of the method for these systems. In particular, we calculate the CD spectrum of the zigzag SWNT (5,0). Figure 6 shows the CD scaled 100 times, where some small features are observed that are associated to numerical errors, which are smaller than 0.1% if they are compared with the signal of chiral SWNTs, as we see below. Again, we confirm that achiral nanotubes do not have optical activity, and that the numerical error associated to the calculation is very small.

Now, let us study the CD of the (4,2) SWNT, where we have found an excellent agreement of the electronic properties and optical absorption with previous theoretical and experimental results.[67–71] The DFT calculated CD spectra of the SWNT (4,2) and its enantiomer, the SWNT (2,4), are shown in Fig. 7. As it should be, CD spectra of (4,2) and (2,4) nanotubes are equal but with opposite sign. Considering the relative intensities of CD of the (5,0) SWNT, shown in Fig. 6, and the (4,2) SWNT, shown in Fig. 7, we find that the numerical error is ~0.1%. This is of the same order of magnitude found in the fullerene section, demonstrating the consistency of the formalism and calculations employed here.

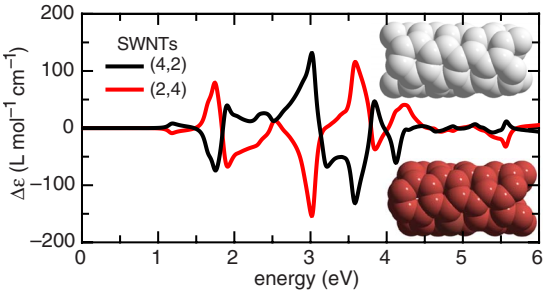

FIG. 7. (Color online) DFT calculated CD spectra of the SWNT (4,2) and its enantiomer, the SWNT (2,4). The spectra have a Gaussian broadening of 0.2 eV. The atomic models of both SWNTs are also shown.

It is well known that the electronic density of states (DOS) is related to optical absorption, and thus, it should be to the CD spectrum. Therefore, we have calculated DOS as a function of energy for the (4,2) nanotube to understand its relationship with CD [see Fig. 8(a)]. Our DOS calculation is in agreement with those obtained by Guo *et al.*[67] who also employed DFT within LDA. For convenience, we have set the Fermi level at 0 eV, thus, below and above of it there are the occupied and empty bands, respectively. In Fig. 8(a), we observed that DOS is characterized by a number of Van Hove singularities, where each peak corresponds to a single-quantum subband. Each Van Hove singularity can be labeled with the index of the subband to which it belongs. The optical transitions occur when the electrons are excited from one occupied energy level to another unoccupied energy level, whose energy we denote by $E_{nn'}$, where n and n' represent the occupied and empty subbands, respectively. In this quasi-one-dimensional (quasi-1D) system, selection rules for electron transitions would depend on the relative polarization of

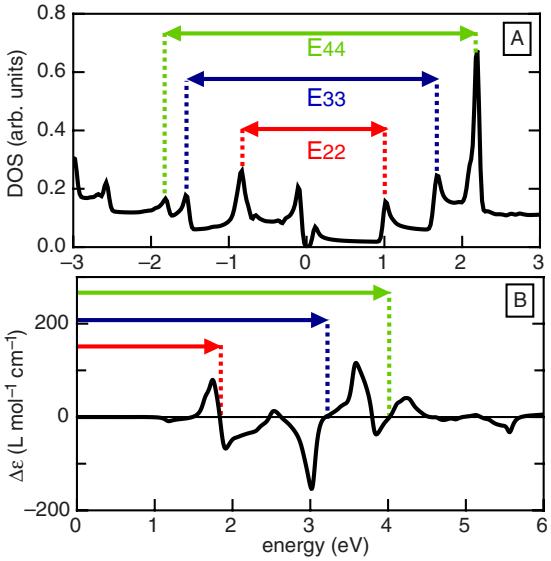

FIG. 8. (Color online) (a) Electronic density of states of nanotube (4,2) as a function of energy. The main parallel optical transition energies E_{nn} are indicated. (b) CD spectrum of nanotube (4,2). The energies of the allowed optical transitions for parallel polarization of light are also indicated.

the electric field vector to respect to the nanotube axis. For instance, for light polarized parallel to the tube axis only symmetrical transitions are allowed, i.e., when $n \rightarrow n$. While for light polarized perpendicularly, optical transitions $n \rightarrow n \pm 1$ are allowed.[72,73] However, perpendicular optical transitions are weak and have not been observed experimentally.[71,74]

In Fig. 8(a), we have indicated the energy difference of the allowed parallel optical transition E_{22}, E_{33}, and E_{44}. In Fig. 8(b), we show the CD spectrum and the correspondent energies associated to such optical transitions. The first energy, $E_{22} \sim 1.9$ eV corresponds to the first important positive-negative structure of the CD, while the negative-positive structure around 3.2 eV is related to the E_{33} transition. Then, again a negative-positive structure at ~ 4 eV is observed and corresponds to E_{44}. The small features at around 1.4 and 2.6 eV seem to be associated to the allowed perpendicular electron transitions.

Ab initio calculations were performed by Chang *et al.*[69] to study the optical transitions of the (4,2) nanotube for circularly polarized light. In this calculation, the authors did not find differences between left and right circular polarizations, and they concluded that this is a consequence of the symmetry of this SWNT. This result is unlikely because the (4,2) nanotube is chiral.[13] On the other hand, they only accounted for the dipolar polarizability difference and not for the rotational strength tensor, which gives CD [see Eq. (8)]. Other quantum-mechanical calculations using a semiempirical tight-binding approach have been performed to study the influence of chirality on the optical properties of SWNTs.[48,49] Both calculations only accounted for π-band electrons, and other important interactions and effects were not included, being unable to handle properly the chiral effects.[50]

Measurements of nanotube diameter and helicity have been made using scanning tunneling microscopy[75–77] and transmission electron microscopy.[78] However, these methods have the disadvantage that nanotubes can be damaged by the energetic incident electron beam used in the probe. Alternatively, nondestructive characterization of SWNTs can be done by using optical spectroscopies such as Raman[79] and fluorescence,[80] which offer a way to determine (n,m). However, it remains a major challenge to establish clearly these parameters, so CD might be a useful tool in this direction. Here, we have demonstrated that CD is directly correlated with Van Hove singularities of DOS, and these depend on the particular structure of each nanotube. Therefore, we can conclude that it might be possible to elucidate the parameters (n,m) for chiral nanotubes that show well-defined CD spectra. We consider that further investigations for a proper interpretation of CD of different SWNTs would be necessary in the near future.

V. SUMMARY AND CONCLUSIONS

A first-principles formalism has been developed to calculate the circular dichroism of chiral structures. The formalism is based in the density-functional theory within the local-density approximation, as well as in the generalized-gradient approximation. Quantum-mechanical expressions for the

macroscopic circular dichroism of finite and periodic structures are obtained from a time-dependent perturbation theory. The formalism has been implemented into the SIESTA code, which allows us to study large-scale finite or periodic nanostructures, such as fullerenes and carbon nanotubes. We test our methodology with achiral systems, where no circular dichroism signal is found, and also using pairs of enantiomers where it is confirmed that both circular dichroism spectra are equal but opposite in sign. The optical activity of the chiral fullerenes C_{76} and C_{78} are studied, finding an excellent agreement with experiments. Our results provide a better description of the circular dichroism of these fullerenes than previously reported semiempirical quantum-mechanical calculations. We also apply the method to calculate the circular dichroism of the high fullerenes C_{90} and C_{100}, which are of the same order of magnitude than the calculated spectra for C_{76} and C_{78}. It is found that the circular dichroism spectrum of each fullerene shows a characteristic line shape, which can be useful to identify their atomic structure. To show the versatility of the formalism, the method is applied to investigate periodic systems such as carbon single-wall nanotubes, and the particular cases of the nanotubes (5,0) and (4,2) are studied. The first nanotube is achiral, so it does not present circular dichroism. On the other hand, the optical activity of the nanotube (4,2) is explained in terms of the electronic density of states. It is conclude that this methodology provides theoretical support for the quantification, understanding, and prediction of chirality and its measurement in nanostructures. The numerical error is smaller than 0.1% in the systems studied here. The methodology can be useful to study a variety of phenomena in the nanoscale such as intrinsic and adsorbate-induced chirality in extended metal surfaces or the origin of optical activity in ligand-protected metallic nanoparticles, and others, as well as the understanding of the interaction between biological systems and organic molecules such as DNA and amino acids, with nanostructures, which are of relevance to understand phenomena associated to nanotoxicology, nanopharmacology, and others. It is expected that this information would be useful to motivate further experimental and theoretical studies, as well as the interpretation of natural optical activity in terms of the electronic circular dichroism of the chirality at the nanoscale.

ACKNOWLEDGMENTS

Partial financial support from CONACyT Grant No. 48521, and DGAPA-UNAM Grant No. IN106408 is also acknowledged.

*Corresponding author: cecilia@fisica.unam.mx

[1] L. Barron, *Molecular Light Scattering and Optical Activity*, 2nd ed. (Cambridge University Press, Cambridge, 2004).
[2] N. Berova, K. Nakanishi, and R. W. Woody, *Circular Dichroism, Principles and Applications*, 2nd ed. (Wiley-VCH, New York, 2000).
[3] S. Mauskopf, *Chiral Analysis* (Elsiever, Amsterdam, 2006).
[4] J. Zhang, M. T. Albelda, Y. Liu, and J. W. Canary, Chirality **17**, 404 (2005).
[5] *Surface and Nanomolecular Catalysis*, edited by R. Richards (CRC, Boca Raton, 2006).
[6] X. López-Lozano, L. A. Pérez, and I. L. Garzón, Phys. Rev. Lett. **97**, 233401 (2006).
[7] X. Peng, N. Komatsu, S. Bhattacharya, T. Shimawaki, S. Aonuma, T. Kimura, and A. Osuka, Nat. Nanotechnol. **2**, 361 (2007).
[8] G. M. Whitesides and B. Grzybowski, Science **295**, 2418 (2002).
[9] H. Fenniri, B. L. Deng, and A. E. Ribbe, J. Am. Chem. Soc. **124**, 11064 (2002).
[10] P. W. Fowler and D. E. Manolopoulos, *An Atlas of Fullerenes* (Clarendon, Oxford, 1995).
[11] E. L. Ivchenko and B. Spivak, Phys. Rev. B **66**, 155404 (2002).
[12] N. C. Seeman and P. S. Lukeman, Rep. Prog. Phys. **68**, 237 (2005).
[13] R. Saito, G. Dresselhaus, and M. S. Dresselhaus, *Physical Properties of Carbon Nanotubes* (Imperial College Press, London, U. K., 1998).
[14] T. G. Schaaff and R. L. Whetten, J. Phys. Chem. B **104**, 2630 (2000).
[15] H. Yao, Curr. Nanosci. **4**, 92 (2008), see references therein.
[16] C. Noguez and I. L. Garzón, Chem. Soc. Rev. (2009), see references therein.
[17] P. D. Jadzinsky, G. Calero, C. J. Ackerson, D. A. Bushnell, and R. D. Kornberg, Science **318**, 430 (2007).
[18] I. E. Santizo, F. Hidalgo, L. A. Pérez, C. Noguez, and I. L. Garzón, J. Phys. Chem. C **112**, 17533 (2008).
[19] A. Lechtken, D. Schooss, J. R. Stairs, M. N. Blom, F. Furche, N. Morgner, and O. Kostko, B. v. Issendorff, and M. M. Kappes, Angew. Chem. Int. Ed. **46**, 2944 (2007).
[20] X. Gu, S. Bulusu, X. Li, X. C. Zeng, J. Li, X. G. Gong, and L. S. Wang, J. Phys. Chem. C **111**, 8228 (2007).
[21] T. D. Crawford, M. C. Tam, and M. L. Abrams, J. Phys. Chem. A **111**, 12057 (2007).
[22] L. Rosenfeld, Z. Phys. **52**, 161 (1928).
[23] D. J. Caldwell and H. Eyring, *The Theory of Optical Activity* (Wiley-Interscience, New York, 1971).
[24] L. D. Barron and C. G. Gray, J. Phys. A: Math. Theor. **6**, 59 (1973).
[25] J. Linderberg and Y. Öhrn, *Propagators in Quantum Chemistry*, 2nd ed. (Wiley, New Jersey, 2004).
[26] D. Sánchez-Portal, P. Ordejón, E. Artacho, and J. M. Soler, Int. J. Quantum Chem. **65**, 453 (1997).
[27] J. M. Soler, E. Artacho, J. D. Gale, A. García, J. Junquera, P. Ordejón, and D. Sánchez-Portal, J. Phys.: Condens. Matter **14**, 2745 (2002).
[28] C. Noguez and S. E. Ulloa, Phys. Rev. B **56**, 9719 (1997).
[29] N. Troullier and J. L. Martins, Phys. Rev. B **43**, 1993 (1991).
[30] J. P. Perdew, K. Burke, and M. Ernzerhof, Phys. Rev. Lett. **77**, 3865 (1996).
[31] URL http://www.cochem2.tutkie.tut.ac.jp/Fuller/higher/higherE.html.

[32] H. W. Kroto, J. R. Heath, S. C. O'Brien, R. F. Curl, and R. E. Smalley, Nature (London) **318**, 162 (1985).
[33] F. Diederich *et al.*, Science **252**, 548 (1991).
[34] F. Diederich, R. L. Whetten, C. Thilgen, R. Ettl, I. Chao, and M. M. Alvarez, Science **254**, 1768 (1991b).
[35] F. Diederich and R. L. Whetten, Acc. Chem. Res. **25**, 119 (1992).
[36] D. E. Manolopoulos and P. W. Fowler, Chem. Phys. Lett. **187**, 1 (1991).
[37] R. Ettl, I. Chao, F. Diederich, and R. L. Whetten, Nature (London) **353**, 149 (1991).
[38] J. M. Hawkins and A. Meyer, Science **260**, 1918 (1993).
[39] J. M. Hawkins, M. Nambu, and A. Meyer, J. Am. Chem. Soc. **116**, 7642 (1994).
[40] R. Kessinger, J. Crassous, A. Herrmann, M. Rüttimann, L. Echegoyen, and F. Diederich, Angew. Chem. Int. Ed. **37**, 1919 (1998).
[41] H. Goto, N. Harada, J. Crassous, and F. Diederich, J. Chem. Soc., Perkin Trans. 2 **1998**, 1719.
[42] C. Noguez, J. Phys. Chem. C **111**, 3806 (2007).
[43] F. Hidalgo and C. Noguez (unpublished).
[44] M. Fanti, G. Orlandi, G. Poggi, and F. Zerbetto, Chem. Phys. **223**, 159 (1997).
[45] A. Jiemchooroj and P. Norman, J. Chem. Phys. **126**, 134102 (2007).
[46] F. Furche and R. Ahlrichs, J. Am. Chem. Soc. **124**, 3804 (2002).
[47] J. Crassous, J. Rivera, N. S. Fender, L. Shu, L. Echegoyen, C. Thilgen, A. Herrmann, and F. Diederich, Angew. Chem. Int. Ed. **38**, 1613 (1999).
[48] S. Tasaki, K. Maekawa, and T. Yamabe, Phys. Rev. B **57**, 9301 (1998).
[49] G. G. Samsonidze, A. Grüneis, R. Saito, A. Jorio, A. G. Souza Filho, G. Dresselhaus, and M. S. Dresselhaus, Phys. Rev. B **69**, 205402 (2004).
[50] A. Sánchez-Castillo, C. E. Román-Velázquez, and C. Noguez, Phys. Rev. B **73**, 045401 (2006).
[51] S. Iijima and T. Ichihashi, Nature (London) **363**, 603 (1993).
[52] D. S. Bethune and C. H. Kiang, M. S. d. Vries, G. Gorman, R. Savoy, J. Vazquez, and R. Veyers, Nature (London) **363**, 605 (1993).
[53] S. M. Bachilo, L. Balzano, J. E. Herrera, F. Pompeo, D. E. Resasco, and R. B. Weisman, J. Am. Chem. Soc. **125**, 11186 (2003).
[54] P. G. Collins, M. S. Arnold, and P. Avouris, Science **292**, 706 (2001).
[55] R. Krupke and F. Hennrich, H. v. Löhneysen, and M. M. Kappes, Science **301**, 344 (2003).
[56] M. S. Strano, C. A. Dyke, M. L. Usrey, P. W. Barone, M. J. Allen, H. Shan, C. Kittrell, R. H. Hauge, J. M. Tour, and R. E. Smalley, Science **301**, 1519 (2003).
[57] M. Zheng, A. Jagota, E. D. Semke, B. A. Diner, R. S. Mclean, S. R. Lustig, R. E. Richardson, and N. G. Tassi, Nature Mater. **2**, 338 (2003a).
[58] H. Li, B. Zhou, Y. Lin, L. Gu, W. Wang, K. A. S. Fernando, S. Kumar, L. F. Allard, and Y.-P. Sun, J. Am. Chem. Soc. **126**, 1014 (2004).
[59] M. S. Arnold, A. A. Green, J. F. Hulvat, S. I. Stupp, and M. C. Hersam, Nat. Nanotechnol. **1**, 60 (2006).
[60] Y. Maeda *et al.*, J. Am. Chem. Soc. **128**, 12239 (2006).
[61] M. Zheng *et al.*, Science **302**, 1545 (2003b).
[62] G. S. Duesberg, J. Muster, V. Krstic, M. Burghard, and S. Roth, Appl. Phys. A: Mater. Sci. Process. **67**, 117 (1998).
[63] E. Farkas, M. E. Anderson, Z. Chen, and A. G. Rinzler, Chem. Phys. Lett. **363**, 111 (2002).
[64] G. Dukovic, M. Balaz, P. Doak, N. D. Berova, M. Zheng, R. S. Mclean, and L. E. Brus, J. Am. Chem. Soc. **128**, 9004 (2006).
[65] X. Peng, N. Komatsu, S. Bhattacharya, T. Shimawaki, S. Aonuma, T. Kimura, and A. Osuka, Nat. Nanotechnol. **2**, 361 (2007b).
[66] X. Peng, N. Komatsu, T. Kimura, and A. Osuka, J. Am. Chem. Soc. **129**, 15947 (2007c).
[67] G. Y. Guo, K. C. Chu, D. S. Wang, and C. G. Duan, Phys. Rev. B **69**, 205416 (2004).
[68] M. Machón, S. Reich, C. Thomsen, D. Sánchez-Portal, and P. Ordejón, Phys. Rev. B **66**, 155410 (2002).
[69] E. Chang, G. Bussi, A. Ruini, and E. Molinari, Phys. Rev. Lett. **92**, 196401 (2004).
[70] A. G. Marinopoulos, L. Reining, A. Rubio, and N. Vast, Phys. Rev. Lett. **91**, 046402 (2003).
[71] Z. M. Li *et al.*, Phys. Rev. Lett. **87**, 127401 (2001).
[72] H. Ajiki and T. Ando, Physica B **201**, 349 (1994).
[73] I. Bozŏvić, N. Bozŏvić, and M. Damnjanović, Phys. Rev. B **62**, 6971 (2000).
[74] S. Reich, C. Thomsen, and J. Maultzsch, *Carbon Nanotubes* (WILEY-VCH Verlag GmbH & Co. KGaA, Berlin, Federal Republic of Germany, 2004).
[75] L. C. Venema, V. Meunier, P. Lambin, and C. Dekker, Phys. Rev. B **61**, 2991 (2000).
[76] L. Tapasztó, G. I. Márk, A. A. Koós, P. Lambin, and L. P. Biró, J. Phys.: Condens. Matter **18**, 5793 (2006).
[77] L. P. Biró, Europhys. Lett. **50**, 494 (2000).
[78] M. Gao, J. M. Zuo, R. D. Twesten, I. Petrov, L. A. Nagahara, and R. Zhang, Appl. Phys. Lett. **82**, 2703 (2003).
[79] S. M. Bachilo, M. S. Strano, C. Kittrell, R. H. Hauge, R. E. Smalley, and R. B. Weisman, Science **298**, 2361 (2002).
[80] C. L. Kane and E. J. Mele, Phys. Rev. Lett. **90**, 207401 (2003).